

Krzysztof Kwieciński, Katarzyna Lota, Marcin Kiełbasiński, Janusz Pikuła, Marek St. Węglowski, Piotr Śliwiński, Sebastian Stano, Michał Urbańczyk, Szymon Kowieski, Piotr Śliwiński, Ewa Jankowska, Rafał Mańczak, Rafał Szostak

Advanced Methods of Joining Battery Cells in the Automotive Industry

Abstract: The article discusses tests performed within a state budget-subsidised research project Research into the Development of Joining Techniques for Battery Packs. The subject of research work includes the selection and development of technologies enabling the joining of battery cells and accumulators used in modern electric cars. The works conducted previously involved the performance of tests related to the joining of cells using ultrasonic welding, resistance welding, laser beam welding, electron beam welding and plasma arc welding. The technologies developed within the project will make it possible to optimize the manufacturing of Polish batteries.

Keywords: laser beam welding, electron beam welding, laser beam, electron beam, vacuum, stainless steel

DOI: [10.17729/ebis.2022.5/2](https://doi.org/10.17729/ebis.2022.5/2)

Introduction

The pursued reduction of CO₂ emission into the atmosphere forces carmakers to develop emission-free means of transport. A significant increase in the production and sales of both hybrid (plug-in) and all-electric cars necessitates increased production capacity as well as better performance, higher reliability and the longer service life of vehicles. One of more important parameters arising from the above-named requirements is the quality of electric joints of individual cells. During operation, wheeled vehicles are exposed to intensive and long lasting

vibration of variable amplitude and frequency, which may result in damage to battery circuits and, consequently, to open or short circuits and, in extreme cases, even to fire [1–5].

The above-named issues inspire research work, the purpose of which was to develop techniques enabling the joining of battery elements. The state-funded project entitled *Research into the Development of Joining Techniques for Battery Packs* aims to develop technologies making it possible to joint cells and batteries used in modern electric cars. Tests concerning the making of joints and aimed to optimise the

mgr inż. Krzysztof Kwieciński, dr inż. Janusz Pikuła, dr inż. Marek St. Węglowski, mgr. inż. Piotr Śliwiński, dr inż. Sebastian Stano, dr. inż. Michał Urbańczyk, mgr inż. Szymon Kowieski – Łukasiewicz – Institute of Welding; dr hab. inż. Katarzyna Lota, dr inż. Ewa Jankowska, Rafał Mańczak – Łukasiewicz – Institute of Non-Ferrous Metals, Poznań division; mgr. inż. Marcin Kiełbasiński, Rafał Szostak – Łukasiewicz – Tele and Radio Research Institute

production of Polish batteries involved the use of ultrasonic welding, resistance welding, laser beam welding, electron beam welding and plasma arc welding processes. The laser beam welding process was performed using a welding station equipped with a TruPulse 103 pulsed laser, enabling the performance of the classical pulsed laser beam process. Further works will include the purchase of a single-mode laser beam welding station featuring a penetration depth measurement system. The electron beam welding process was performed using an XW150:30/756 welding and surface processing machine. The plasma arc welding process will be performed using a station provided with an MSP 51 plasma supply system and an Eu Tronic Gap 3001 welding unit. The ultrasonic welding process has been performed using a Sonic Welder ultrasonic welding machine featuring ultrasonic systems (Łukasiewicz – Tele and Radio Research Institute). The project will involve the making of five tools used for the welding of battery packs containing variously-shaped welds and the recording of process parameters during the performance of technological welding tests [1].

The optimisation of techniques used to join materials used in fastening elements of battery packs requires the development and the verification of numerical models of pressure and fusion welding processes in relation to selected configurations of elements being joined. Numerical (thermal) models enabling the simulation of temperature fields will involve the use of the SysWeld and the Sorpas environments. The final result will consist in the development of complete numerical (thermal) models making it possible to determine the temperature of elements being joined in relation to pressure and fusion welding process parameters characteristic of a given joining method. The models will enable the development of technologies making it possible to join selected fastening elements in relation to geometrical dimensions and structural materials.

All of the tasks have been performed within collaboration involving Łukasiewicz – Institute of Welding, Łukasiewicz – Tele and Radio Research Institute and Łukasiewicz – Institute of Non-Ferrous Metals, Poznań division.

Project implementation

The current stage of the project involved the development of FEM-based numerical models (using the SYSWELD software programme) concerning the welding of battery terminals. The calculations were performed to identify the effect of welding process parameters and technological solutions on the field of temperature, the dimensions of the weld and the generation of welding stresses and strains (distortions). The tests involved analysis concerning laser welding processes performed using various parameters as well as related to the making of a series of test joints using the electron beam welding and laser beam welding processes.

FEM-based numerical simulations of single spot laser beam welding

The first preparatory stage, concerning the numerical model of the laser beam welding process, involved the spot welding process. The numerical model included actual laser beam welding process parameters, i.e. a power of 450 W and an impulse duration of 4 ms. The CAD geometry, used to prepare the mesh of finite elements, was based on dimensions of an actual element (Fig. 1). The thickness of stamped



Fig. 1. Element subjected to laser beam welding

sheets amounted to 0.15 mm. The material data used in the simulation process were those of steel grade S355.

The mesh of finite elements (Fig. 3) was prepared using CAD geometry (presented in Figure 2). The mesh was concentrated in crucial areas (areas of direct heat effect resulting from the welding process in the central part of the element). The material properties attributed to the finite elements were consistent with related assumptions.

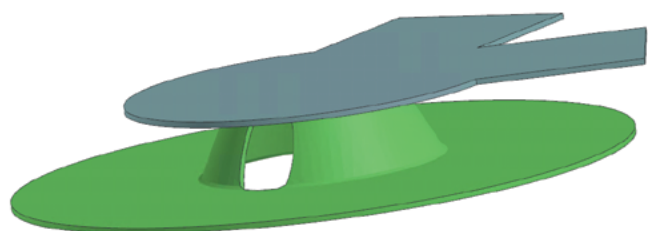


Fig. 2. CAD geometry used in the making of the mesh of finite elements

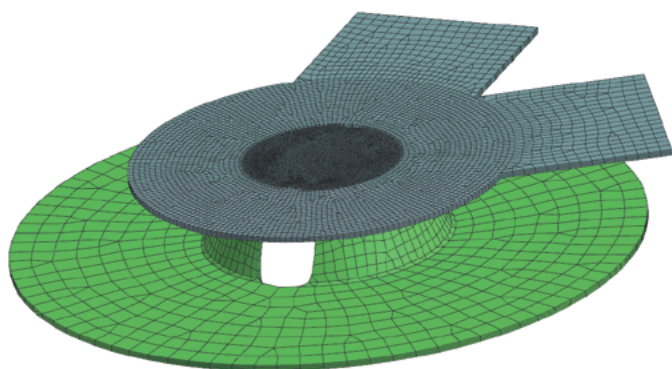


Fig. 3. Mesh of finite elements in the FEM-based model of the laser beam welding process

The model involved the exchange of heat (convection and thermal radiation) with the environment. Because of the fact that the formation of the weld pool during laser beam welding is a complex phenomenon, a volumetric heat source (e.g. of cylindrical geometry – see Fig. 4) is used both in engineering and scientific practice. The heat source diameter was consistent with the dimensions of the laser beam and amounted to 0.4 mm. The laser beam effect (heat input to specific material volume) was defined at a depth of 0.15 mm (which was connected with the direct heating of the upper sheet).

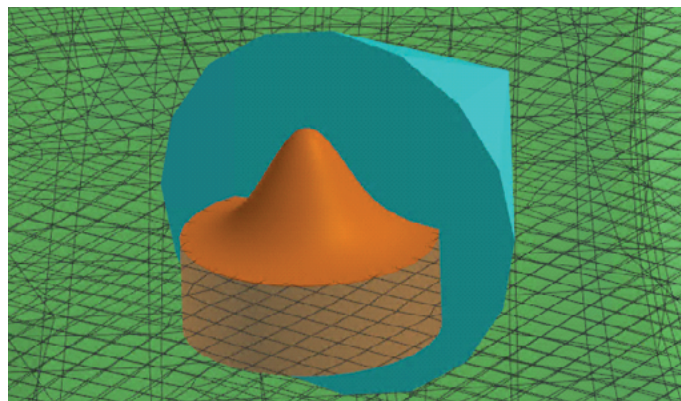


Fig. 4. Cylindrical heat source used in the numerical model

The programme of the tests involved changes of laser beam power values and those of the coefficient of heat exchange in the contact area between the upper and the lower element. The tests included the identification of the effect of the above-named parameters on the geometry (width and height of the melted area) and the maximum temperature at the central point of the weld of the lower part of the lower sheet (Fig. 5). The area treated as melted was the one where the value of temperature exceeded 1450°C.

The programme of the single spot laser beam welding process involving FEM-based qualitative analysis is presented in Table 1. The parameters adopted in the initial model were the following:

- laser beam power: 450 W,
- coefficient of heat exchange in the contact area: 0.092.

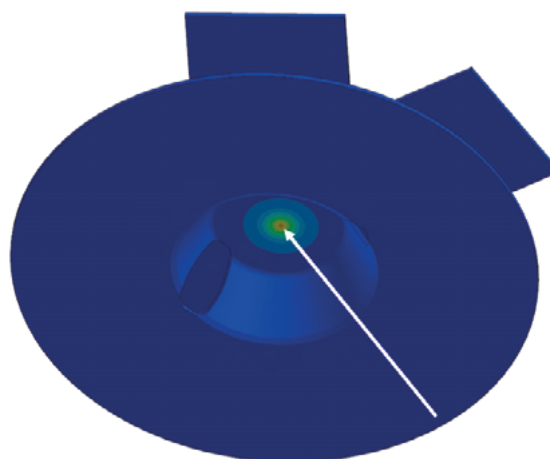


Fig. 5. Central point of the weld on the lower surface of the lower sheet (maximum temperature measurement point)

Table 1. Programme of single spot laser beam welding involving FEM-based modelling

Model	Laser beam power, W	Coefficient of heat exchange coefficient in the contact area, -
1	720	0.092
2	630	0.092
3	540	0.092
4	450	0.092
5	360	0.092
6	270	0.092
7	180	0.092
8	450	0.147
9	450	0.129
10	450	0.110
11	450	0.074
12	450	0.055
13	450	0.037

The qualitative analysis performed using the models with one weld aimed to define the effect of analysed parameters (power and contact coefficient) on the field of temperature. Selected results depicting the main view from the upper and the lower side of the cross-section of the weld are presented in Table 3.

The tests concerning the effect of the laser beam on the field of temperature in the welded joint area were performed using models 1–7 (Table 1). The obtained field of temperature revealed that a decrease in laser beam power was accompanied by changes of weld geometry (with respect to dimensions) and by decreased penetration in the lower sheet. Model 1–5 revealed penetration in the lower sheet. In turn, in cases of models 6–7, thermal energy was insufficient to obtain penetration in the lower sheet (Table 3). A decrease in laser beam power was accompanied by a decrease in the maximum diameter of the melted area and by a decrease in the maximum penetration, both in the upper and in the lower sheet (Fig. 6 and 7).

In the above-presented analyses, the difference between the highest (model 1, 720 W) and the lowest (model 7, 180 W) laser beam power amounted to 300%. In turn, the difference between the longest measured maximum diameter of the melted area in the upper sheet (model 1, 720 W) and the shortest diameter of the same area (model 7, 180 W) amounted to 67.4%. Without taking into

Table 2. Calculated field of the maximum temperature during the laser beam welding process (1 weld)

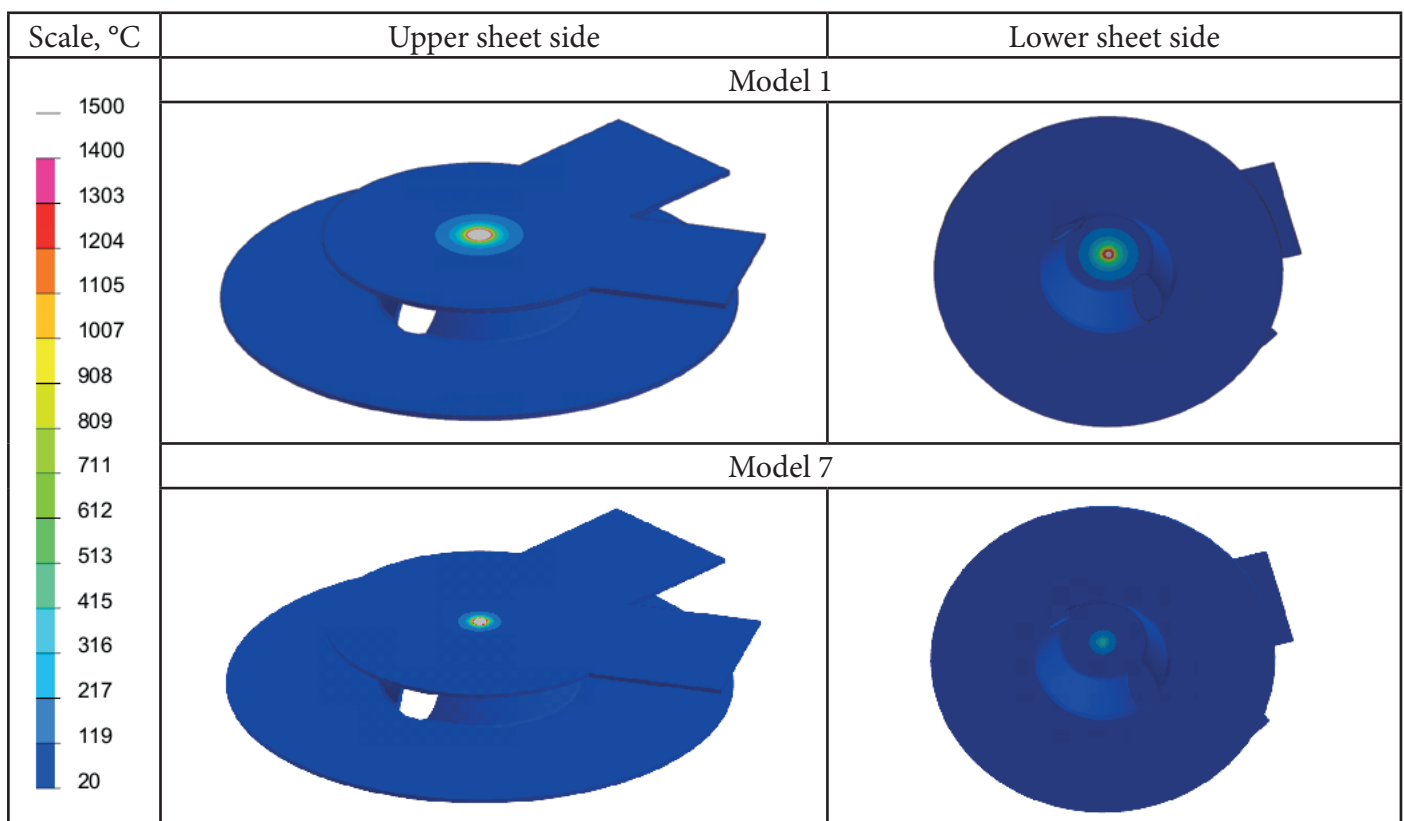
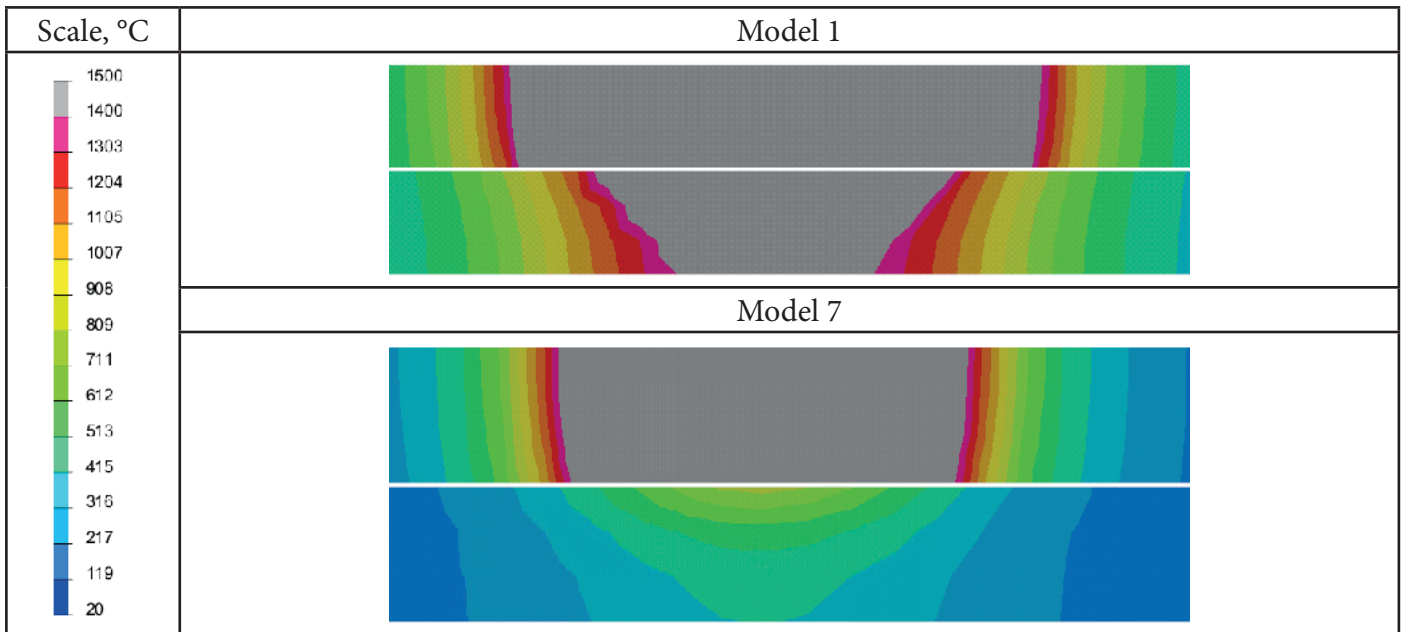


Table 3. Cross-section of the calculated field of the maximum temperature during the laser beam welding process (1 weld)



consideration the results obtained in relation to models 6 and 7 (270 W and 180 W respectively), i.e. not containing the area of the lower sheet penetration, the difference between the highest measured maximum temperature of the area melted in the lower sheet (model 1, 720 W) and the lowest temperature of the same area (model 5, 360 W) amounted to 100%. The difference between the greatest (model 1, 720 W) and the smallest measured penetration (models 6 and 7, 270 W and 180 W respectively) amounted to 100% (Fig. 7).

The maximum temperature (Fig. 8) measured at the central point of the weld on the lower surface of the lower sheet (Fig. 5) was obtained using a beam power of 720 W, whereas the lowest temperature was obtained using a beam power of 720 W 180 W. The temperature measured in models 1 and 2 (720 W and 630 W respectively) was higher than the previously assumed melting point (Fig. 8 and Table 3). The lowest temperature, amounting to 420°C, was measured in model 7 (beam power of 180 W). The comparison of the models without the full penetration across the entire thickness of the two sheets subjected to joining (models 3–7) revealed that the difference between the highest (model 3, 540 W) and the lowest maximum

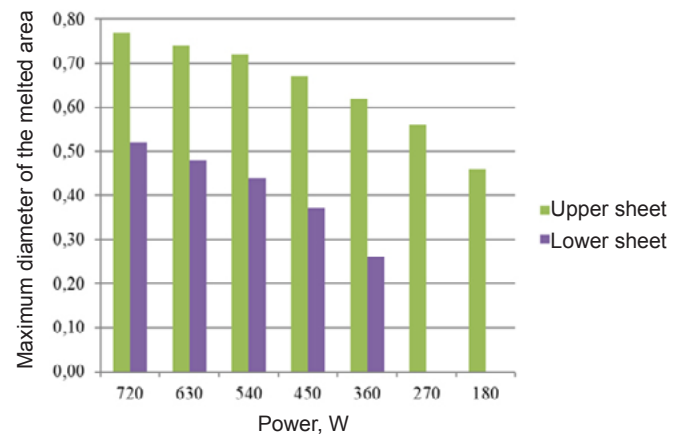


Fig. 6. Maximum diameter of the melted area in the upper and lower sheet, in the models with preset beam power restricted within the range of 720 W to 180 W (models 1–7)

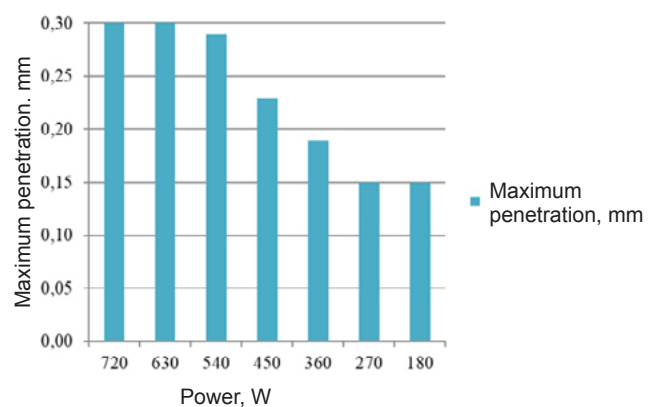


Fig. 7. Maximum penetration (including the thickness of the upper and the lower sheet) in the models with preset beam power restricted within the range of 720 W to 180 W (models 1–7)

temperature at the central point of the weld (model 7, 180 W) amounted to 220.5%.

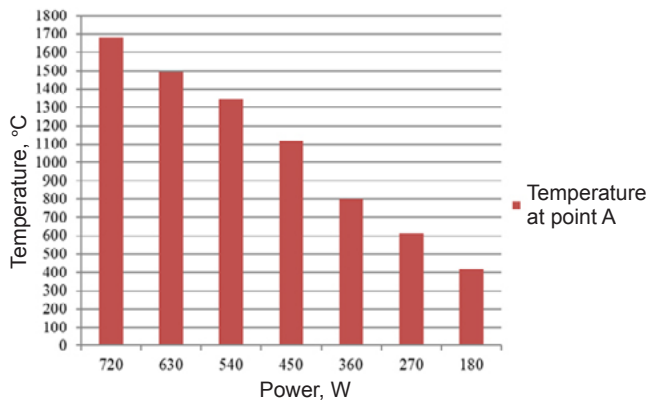


Fig. 8. Maximum temperature measured at the central point of the weld on the lower surface of the lower sheet (in accordance with Fig. 5) in the models with present beam power restricted within the range of 720 W to 180 W (models 1–7)

Actual test joints

The subsequent stage of the research work involved making a series of test joints using both the laser beam and the concentrated electron beam processes. The test joints are presented in Figures 9 and 10. The joints were subjected to tests aimed to compare the results of the experimental tests with the results obtained during numerical modelling.

Conclusions

The above-presented tests and results justified the conclusion of the following remarks concerning the cases subjected to analysis:

- increase in laser beam energy was accompanied by an increase in the length of the diameter of the melted area. The difference between

the longest and shortest measured diameters of the melted area in the upper sheet (models 1 and 7) amounted to 67.4%.

- increase in laser beam energy was accompanied by an increase in the depth of penetration. The highest difference between the maximum largest and smallest penetration (models 1 as well as 6 and 7) amounted to 100%. In all of the above-named cases it was possible to observe the full penetration of the upper sheet. In addition, in relation to a beam power of 720 W and 630 it was possible to observe the full penetration of the lower sheet. In turn, in relation to a beam power of 270 W and 180 W, the lower sheet did not contain any melted area. In relation to a beam power of 540 W, 450 W and 360 W it was possible to observe penetration in the lower sheet. However, the aforesaid penetration was not full (as regards the melting of the material on the lower surface of the lower sheet).
- in tests concerning the effect of laser beam power on the welded joint, in the models involving the application of a beam power of 720 W and 630 W, the maximum temperature at the point subjected to analysis (the central point of the weld on the lower surface of the lower sheet, Fig. 5) was higher than the previously assumed melting point. In the models related to a beam power of 270 and 180 W, the maximum temperature did not exceed 615°C.

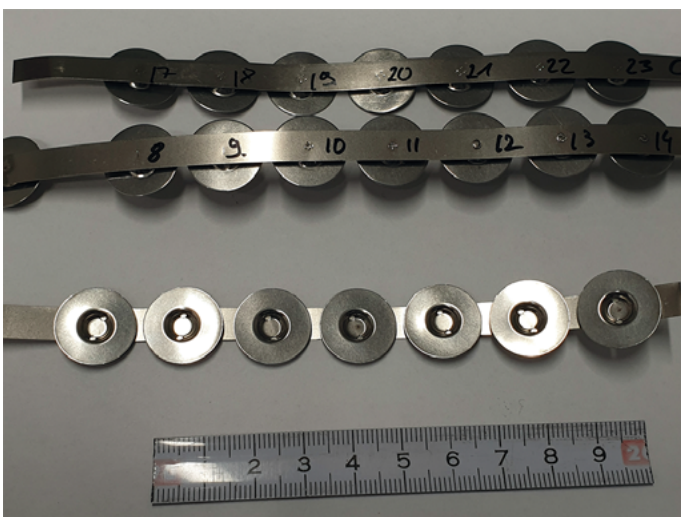


Fig. 9. Laser beam welded joints

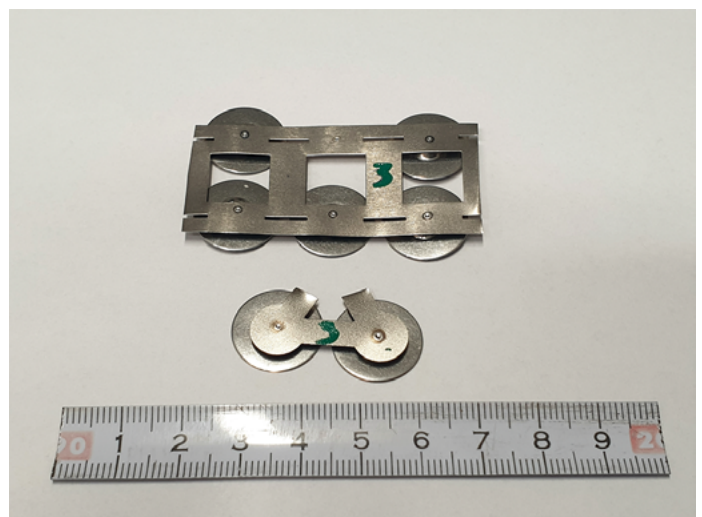


Fig. 10. Electron beam welded joints

In the models where it was possible to observe incomplete penetration of the lower sheet, the maximum temperature at the point subjected to analysis amounted to 1346°C (model 540 W), 1116°C (model 450 W) and 802°C (model 360 W).

Acknowledgements

The Authors wish to express their thanks for funding provided by the Łukasiewicz Research Network, Poland. The research work has been performed within a state-funded project entitled *Research into the Development of Joining Techniques for Battery Packs*.

References

- [1] Kwieciński K., Lota K., Kielbasiński M., Piłkuła J., Śliwiński P., Kubik K., Stano S., Kowieski S., Janowska E., Manczak R.: Experiences in joining cell packs used in the automotive industry. MTS Conference: Materials Technologies in Silesia. 12-15.06.2020 Wisła, Polska.
- [2] Shawn Lee S., Tae H. Kim, Jack Hu S., Cai W.W., Abell A. J.: Joining Technologies for Automotive Lithium-ION Battery Manufacturing – A Review. Proceedings of the ASME 2010 International Manufacturing Science and Engineering Conference. October 12–15, 2010, Erie, Pennsylvania, USA.
- [3] Das D., Ashwin T.R., Barai A.: Modelling and characterisation of ultrasonic joints for Li-ion batteries to evaluate the impact on electrical resistance and temperature raise. *Journal of Energy Storage*, 2019, vol. 22, pp. 239–248.
- [4] Zwicker M.F.R., Moghadama M., Zhang W., Nielsena C.V.: Automotive battery pack manufacturing – a review of battery to tab joining. *Journal of Advanced Joining Processes*, 2020, vol. 1, 100017.
- [5] Schmitz P.: Comparative Study on Pulsed Laser Welding Strategies for Contacting Lithium-Ion Batteries. *Advanced Materials Research*, 2016, vol. 1140, pp. 312–319.
- [6] Mantra P.S., Routara B.Ch., Sahoo S.K.: Weldability appraisalment of dissimilar metal joints: application of ultrasonic spot welding to Li-ion batteries. *Modern Manufacturing Processes*, 2020, pp. 43–68.